

Unique electronic state in ferromagnetic semiconductor FeCl₂ monolayer

Di Lu,^{1,2} Lu Liu,^{1,2} Yaozhenghang Ma,^{1,2} Ke Yang,^{3,1} and Hua Wu^{1,2,4}

¹Laboratory for Computational Physical Sciences (MOE), State Key Laboratory of Surface Physics, and Department of Physics, Fudan University, Shanghai 200433, China

²Shanghai Qi Zhi Institute, Shanghai 200232, China

³College of Science, University of Shanghai for Science and Technology, Shanghai 200093, China

⁴Collaborative Innovation Center of Advanced Microstructures, Nanjing 210093, China

Two-dimensional (2D) van der Waals (vdW) magnetic materials could be an ideal platform for ultracompact spintronic applications. Among them, FeCl₂ monolayer in the triangular lattice is subject to a strong debate. Thus, we critically examine its spin-orbital state, electronic structure, and magnetic properties, using a set of delicate first-principles calculations, crystal field level analyses, and Monte Carlo simulations. Our work reveals that FeCl₂ monolayer is a ferromagnetic (FM) semiconductor in which the electron correlation of the narrow Fe 3*d* bands determines the band gap of about 1.2 eV. Note that only when the spin-orbit coupling (SOC) is properly handled, the unique $d^{5\uparrow}l_{z+}^{\downarrow}$ electronic ground state is achieved. Then, both the orbital and spin contributions (0.59 μ_B plus 3.56 μ_B) to the total magnetic moment well account for, for the first time, the experimental perpendicular moment of 4.3 μ_B/Fe . Moreover, we find that a compressive strain further stabilizes the $d^{5\uparrow}l_{z+}^{\downarrow}$ ground state, and that the enhanced magnetic anisotropy and exchange coupling would boost the Curie temperature (T_C) from 25 K for the pristine FeCl₂ monolayer to 69-102 K under 3%-5% compressive strain. Therefore, FeCl₂ monolayer is indeed an appealing 2D FM semiconductor.

I. INTRODUCTION

Reduced dimensionality and interlayer couplings of bulk vdW materials trigger intriguing electronic, optical and other quantum properties [1–5]. According to the Mermin-Wagner theorem [6], long-range magnetic order at finite temperature is prohibited in 2D isotropic Heisenberg spin-rotational-invariant systems. However, magnetic anisotropies can break spin-rotation symmetry, thus bringing about possible long-range magnetism. Recently, 2D vdW magnets with tunable magnetic anisotropy have attracted a large volume of attention as 2D FM was observed in atomically thin CrI₃ [7] and Cr₂Ge₂Te₆ [8]. These 2D vdW magnets exhibit appealing properties, such as the magnetic anisotropy [9–11], the exotic quantum spin liquid states [12] and antiferromagnetic (AF) topological insulators [13–15]. The abundant properties open a new avenue to spintronic applications, such as spin valves [16], spin filters [17, 18], and data storage [19]. Moreover, owing to the layered structure, one could be able to control the 2D magnetic properties by strain [10, 11], doping [20, 21], heterostructure [22, 23] or applying magnetic/electric field [24, 25]. For example, the T_C of monolayer Fe₃GeTe₂ can exceed room temperature via ionic gating.

The binary transition metal dihalides MX₂ (M = transition metal; X = halogen: Cl, Br, I) are vdW layered materials containing a triangular lattice of M²⁺ cations [26]. The bulk magnetism was analyzed several decades ago [27–30]. Very recently, FeCl₂ monolayer has been synthesized by molecular-beam epitaxy [31, 32], and it is a new 2D vdW magnet with a semiconducting gap of about 1.2 eV [32]. However, several theoretical studies suggest that it is a high-spin ($S = 2$) half-metallic (HM) ferromagnet with a conducting down-spin t_{2g} channel in the local octahedral coordination [33–37]. Another two

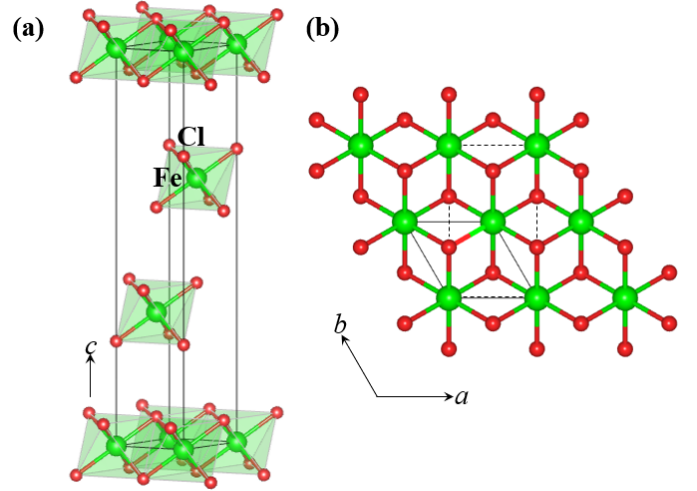


FIG. 1. (a) The crystal structure of FeCl₂ bulk and (b) FeCl₂ monolayer: the solid diamond represents the unit cell, and the dashed rectangular $1 \times \sqrt{3}$ supercell models the stripe AF state.

studies present the FM insulating solution [38, 39], but the ground state was not yet firmly determined through total energy calculations. Moreover, the orbital singlet solution $d^{5\uparrow}a_{1g}^{\downarrow}$ was obtained when the reasonable U and SOC parameters were used [39]. Then, only the spin moment is expected, and it should be smaller than 4 μ_B per Fe²⁺ ($S = 2$) reduced by the Fe-Cl covalence; and a small orbital moment, if any, would be in the plane (see more below, e.g. Table 1). Note that FeCl₂ bulk was reported to have interlayer AF but intralayer FM couplings, with the Néel temperature $T_N = 24$ K and a perpendicular magnetic moment of 4.3 μ_B exceeding the spin-only value [27, 29, 30]. So far, the intralayer

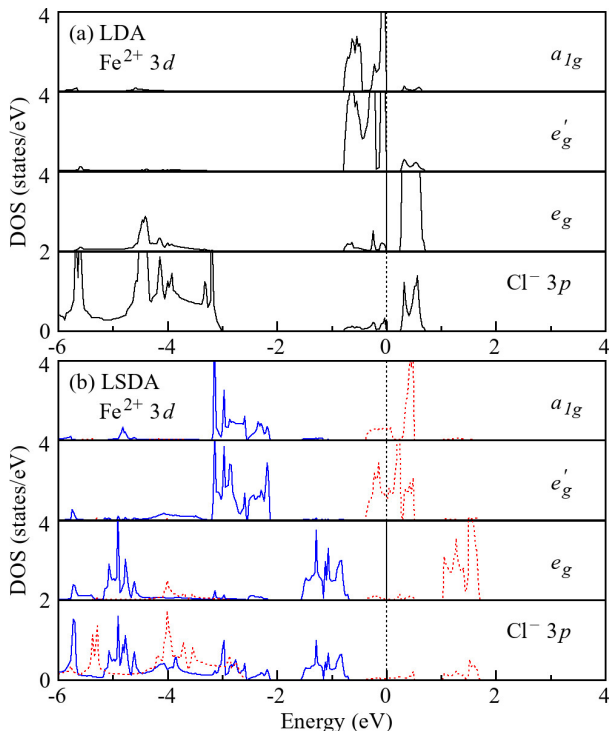


FIG. 2. The DOS results of (a) LDA and (b) LSDA for FeCl₂ monolayer. The blue (red) curves refer to the majority (minority) spin. The Fermi level is set at the zero energy.

FM coupling of most concern for FeCl₂ monolayer has been discussed in the FM HM solution in the previous studies [34, 36, 37], in which the T_C was too much overestimated by the fictitious itinerant magnetism, instead of the true superexchange in this FM semiconducting monolayer. Therefore, the FM semiconducting behavior of FeCl₂ monolayer and the perpendicular magnetic moment remain largely unresolved.

In this work, we critically examine the electronic and magnetic structures of FeCl₂ monolayer using a set of delicate first-principles calculations, crystal field level analyses, and Monte Carlo simulations. Our calculations find a moderate t_{2g} - e_g crystal field splitting for the Fe 3d states, and thus a high-spin ($S = 2$) Fe²⁺ state is achieved by the Hund exchange. Moreover, under the global trigonal crystal field, Fe 3d t_{2g} triplet splits and the e'_g doublet is lower than a_{1g} singlet by 30 meV. Owing to the strong correlation effect of the narrow Fe 3d bands in the triangular lattice, the band gap is determined by the Hubbard U . But note that here the orbital states must be delicately handled, and only when the SOC is properly included, the correct electronic ground state $d^{5\uparrow}l_{z+}^{\downarrow}$ would be achieved. Then, an out-of-plane orbital moment, strong perpendicular magnetic anisotropy of single ion type, and intralayer FM coupling, all well account for the FM semiconducting behavior of FeCl₂ monolayer, with $T_C = 25$ K being estimated by our Monte Carlo simulations. Furthermore, we predict that the $d^{5\uparrow}l_{z+}^{\downarrow}$ ground

state can be further stabilized by a compressive strain, and -3% (-5%) strain would raise the T_C to 69 K (102 K). Therefore, FeCl₂ monolayer is indeed an appealing 2D FM semiconductor.

II. COMPUTATIONAL DETAILS

Density functional theory (DFT) calculations were carried out using the full-potential augmented plane wave plus local orbital code (Wien2k) [40]. The optimized lattice parameter of FeCl₂ monolayer is $a = b = 6.708$ Å, which is close to (within 1.5%) the experimental value of 6.809 Å for the bulk [27]. A vacuum slab of 15 Å was set along the c -axis. The muffin-tin sphere radii were chosen to be 2.2 bohr for Fe atoms and 1.8 bohr for Cl. The plane-wave cut-off energy of 12 Ry was set for the interstitial wave functions, and a $12 \times 12 \times 1$ k-mesh was sampled for integration over the Brillouin zone. To describe the electron correlation effect, several methods may be used, e.g., the local spin density approximation plus Hubbard U (LSDA+ U) method [41], the self interaction correction [42, 43], the hybrid functional [44, 45], and the GW theory [46]. Here the economic and practical LSDA+ U method was employed, with the common values of Hubbard $U = 4.0$ eV and Hund exchange $J_H = 0.9$ eV for Fe 3d electrons. As seen below, our LSDA+SOC+ U calculations well reproduce the experimental band gap, which also justifies the choice of the U value. The SOC is included for both Fe 3d and Cl 3p orbitals by the second-variational method with scalar relativistic wave functions. We critically examine the orbital states and hence determine the correct electronic ground state by calculating the crystal field level splittings and by comparing orbital multiplets using total energy calculations. For this purpose, we perform DFT calculations using spin-restricted LDA, spin-polarized LSDA, LSDA+ U , and LSDA+SOC+ U , as detailed below. Moreover, we perform Monte Carlo simulations on a $8 \times 8 \times 1$ spin matrix to estimate the T_C of FeCl₂ monolayer, using the Metropolis method [47] and the obtained exchange parameter and magnetic anisotropy from the LSDA+SOC+ U calculations.

III. RESULTS AND DISCUSSION

We first analyze the crystal field levels of the Fe²⁺ ion in FeCl₂ monolayer, which is crucial for understanding of the electronic ground state. As seen in Fig. 1, FeCl₂ monolayer adopts the 1- T structure with $P\bar{3}m1$ space group [31]. Each Fe²⁺ ion is surrounded by six Cl⁻ ions, thus forming an FeCl₆ octahedron, and the edge-sharing octahedra comprise a triangular lattice. The local octahedral crystal field splits the Fe 3d orbitals into the lower-lying t_{2g} triplet and higher e_g doublet. The t_{2g} triplet further splits into the e'_g doublet and the a_{1g} singlet in the global trigonal crystal field. The global coordinate

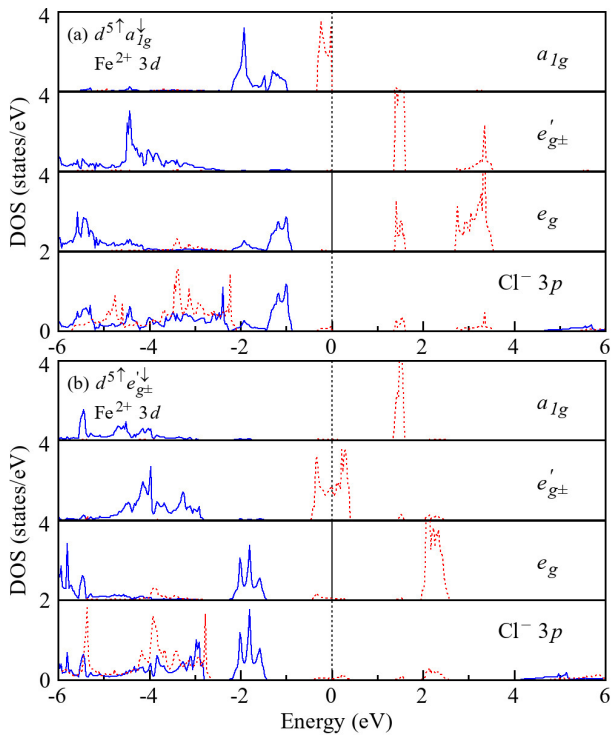


FIG. 3. The DOS results of LSDA+ U for (a) the semiconducting $d^{5\uparrow}a_{1g}^{\downarrow}$ state and (b) the half-metallic $d^{5\uparrow}e'_{g\pm}$ state. The blue (red) curves refer to the majority (minority) spin. The Fermi level is set at the zero energy.

system was used in the following calculations, with the z axis along the $[111]$ direction of the local FeCl_6 octahedron and y along the $[1\bar{1}0]$ direction [48, 49].

To see the crystal field effect, we first perform the spin-restricted LDA calculation. Our results show that the t_{2g} - e_g octahedral crystal field splitting is about 1 eV, see Fig. 2(a). Among the t_{2g} , the a_{1g} singlet and e'_g doublet are almost degenerate at a first look. In reality, by a close look the e'_g is found to be slightly lower than the a_{1g} by 30 meV, by calculating the center of gravity of their respective partial density of states (DOS). This result is crucial for the following discussion of the correct electronic ground state. The $\text{Cl } 3p$ state mainly lies in the range of 3-6 eV below the Fermi level, and its strong $pd\sigma$ hybridization with $\text{Fe } 3d$ - e_g and weak $pd\pi$ hybridization with $\text{Fe } 3d$ - t_{2g} are both evident.

Apparently, the $\text{Fe } 3d$ orbitals form narrow bands in the triangular lattice, with the bandwidth less than 1 eV. Therefore, these localized $3d$ orbitals would be strongly spin-polarized by the local Hund exchange. Through the spin-polarized LSDA calculation, we find that indeed the Fe^{2+} ion is in the high-spin $S = 2$ state, see Fig. 2(b). The up-spin $3d$ orbitals are fully occupied, and the down-spin t_{2g} (a_{1g} and e'_g) is 1/3 partially occupied, seemingly giving a HM solution. Note that this HM solution is fictitious, as the strong correlation effect of the narrow bands is absent in the LSDA calculations and in reality FeCl_2 monolayer has a semiconducting gap of about 1.2

TABLE I. Relative total energies ΔE (meV/fu) for FeCl_2 monolayer in different states and under different strains by LSDA+ U and LSDA+SOC+ U , and the local spin and orbital moments (μ_B) for the Fe^{2+} ion. The FM state is considered in most calculations except for those marked with stripe AF, and \perp (\parallel) represents the out-of-plane (in-plane) magnetization.

	States	ΔE	M_{spin}	M_{orb}	
LSDA+ U	$d^{5\uparrow}a_{1g}^{\downarrow}$	0.00	3.55	—	
	$d^{5\uparrow}e'_{g\pm}$	161.66	3.58	—	
LSDA+SOC+ U	$d^{5\uparrow}L_{z^+}^{\downarrow}, \perp$	0.0	3.56	0.59	
	$d^{5\uparrow}L_{z^+}^{\downarrow}, \perp$ (AF)	2.83	± 3.54	± 0.62	
	$d^{5\uparrow}L_{z^+}^{\downarrow}, \parallel$	13.43	3.56	0.20	
	$d^{5\uparrow}a_{1g}^{\downarrow}, \parallel$	84.83	3.54	0.23	
	$d^{5\uparrow}a_{1g}^{\downarrow}, \perp$	91.48	3.54	0.01	
	-5%	$d^{5\uparrow}L_{z^+}^{\downarrow}, \perp$	0.00	3.53	0.71
		$d^{5\uparrow}L_{z^+}^{\downarrow}, \perp$ (AF)	17.13	± 3.51	± 0.76
		$d^{5\uparrow}L_{z^+}^{\downarrow}, \parallel$	18.12	3.53	0.20
	-3%	$d^{5\uparrow}a_{1g}^{\downarrow}, \parallel$	96.97	3.53	0.20
		$d^{5\uparrow}L_{z^+}^{\downarrow}, \perp$	0.00	3.54	0.67
$d^{5\uparrow}L_{z^+}^{\downarrow}, \perp$ (AF)		10.39	± 3.52	± 0.71	
3%	$d^{5\uparrow}L_{z^+}^{\downarrow}, \parallel$	16.08	3.54	0.24	
	$d^{5\uparrow}a_{1g}^{\downarrow}, \parallel$	92.09	3.53	0.23	
	$d^{5\uparrow}L_{z^+}^{\downarrow}, \perp$	2.41	3.57	0.51	
	$d^{5\uparrow}L_{z^+}^{\downarrow}, \perp$ (AF)	0.00	± 3.56	± 0.54	
5%	$d^{5\uparrow}L_{z^+}^{\downarrow}, \parallel$ (AF)	11.94	± 3.55	± 0.24	
	$d^{5\uparrow}a_{1g}^{\downarrow}, \parallel$ (AF)	68.61	± 3.52	± 0.32	
	$d^{5\uparrow}L_{z^+}^{\downarrow}, \perp$	5.00	3.58	0.46	
	$d^{5\uparrow}L_{z^+}^{\downarrow}, \perp$ (AF)	0.00	± 3.57	± 0.47	
	$d^{5\uparrow}L_{z^+}^{\downarrow}, \parallel$ (AF)	9.11	± 3.56	± 0.34	
	$d^{5\uparrow}a_{1g}^{\downarrow}, \parallel$ (AF)	52.05	± 3.54	± 0.46	

eV [32].

Now we carry out LSDA+ U calculations to elucidate the electron correlation effect. As seen in Fig. 3, we obtain two contrasting high-spin solutions, one with the down-spin a_{1g} occupation, and the other with the down-spin e'_g half filling. Apparently, the former solution has a semiconducting gap of 1.42 eV (well comparable with the experimental one of about 1.2 eV [32]), while the latter one is again half metallic. Note that although the e'_g doublet is lower than the a_{1g} singlet in the crystal field level diagram as discussed above, the down-spin e'_g doublet has to be half filled for the high-spin Fe^{2+} ion due to the present symmetry constriction. Thus, this solution has to be computationally half metallic, even with strong correlation effect which is sufficient to open a band gap. Owing to the half filling of the narrow e'_g band which strides over the Fermi level, this half-metallic solution is less stable, by about 162 meV/fu in our LSDA+ U calculations (see Table 1), than the semiconducting solution with the down-spin a_{1g} occupation. The present LSDA+ U results show that the experimental band gap is determined by the Hubbard U . Then one may assume that the semiconducting solution with the down-spin a_{1g} occupation is the correct one. However, this solution is an orbital singlet, and in principle it has no orbital moment but just a spin

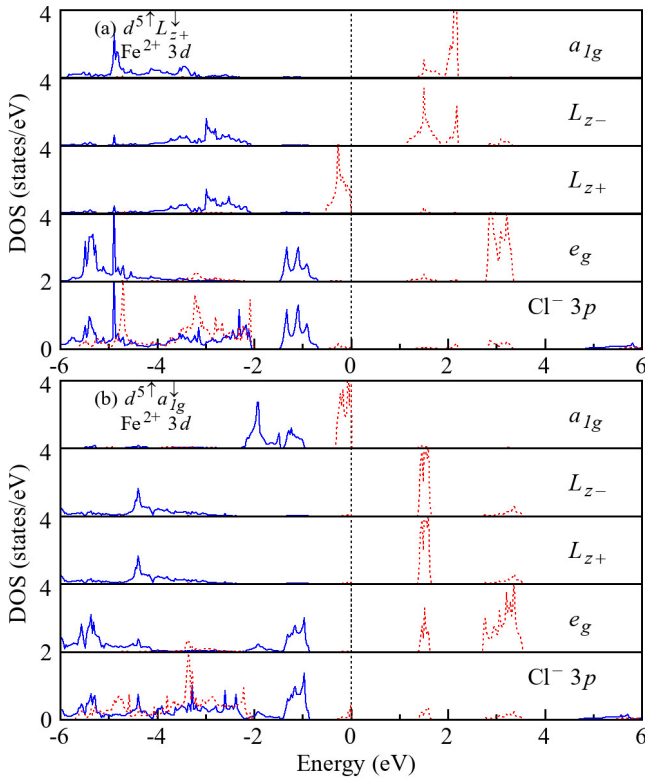


FIG. 4. The DOS results of LSDA+SOC+ U for (a) the $d^{5\uparrow}l_{z+}^{\downarrow}$ ground state and (b) the $d^{5\uparrow}a_{1g}^{\downarrow}$ metastable state. The blue (red) curves stand for the majority (minority) spins. The Fermi level is set at the zero energy.

moment ($3.55 \mu_B/\text{Fe}$, see Table 1) for the high-spin $S = 2$ state. Even considering the SOC mixing between the nearly degenerate a_{1g} and e'_g (see below), a small in-plane orbital moment is expected for this solution. Then this semiconducting solution with the down-spin a_{1g} occupation cannot account for the experimental perpendicular magnetic moment of $4.3 \mu_B$ [27, 29, 30]. In this sense, this semiconducting $d^{5\uparrow}a_{1g}^{\downarrow}$ solution is not the correct ground state.

The Hubbard U determines the band gap of FeCl_2 monolayer and produces a strong orbital polarization for the down-spin t_{2g} (a_{1g} and e'_g) states. In order to find the correct electronic ground state, one needs to delicately handle the orbital degrees of freedom. When the SOC is included, the e'_g doublet splits into l_{z+} and l_{z-} states, with the respective orbital moments of $+1 \mu_B$ and $-1 \mu_B$ along the z axis (i.e., the crystallographic c axis). Then the (near) degeneracy of the t_{2g} states is completely lifted upon the SOC effect, and each of them can now be subject to an orbital polarization by the Hubbard U . We now perform the LSDA+SOC+ U calculations and carefully handle the orbital multiplets, see Table 1. In particular, we now find the $d^{5\uparrow}l_{z+}^{\downarrow}$ ground state, and it is semiconducting with a band gap of 1.17 eV (very close to the experimental one of about 1.2 eV [32]), see Fig. 4(a). By a simple comparison between this semiconduct-

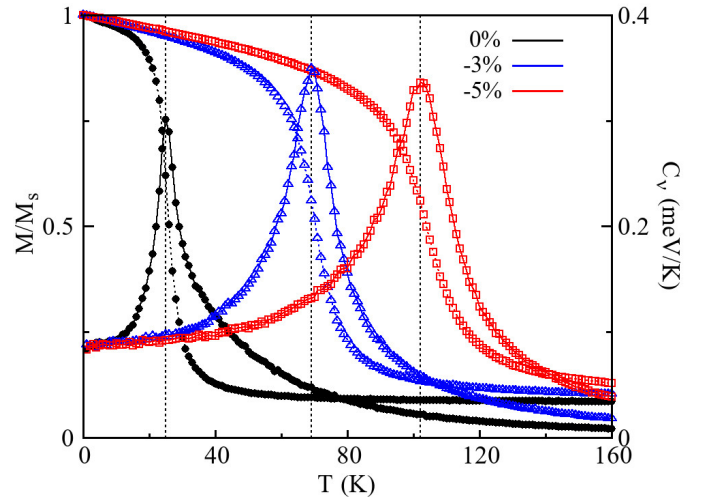


FIG. 5. Monte Carlo simulations of the magnetization and the magnetic specific heat for FeCl_2 monolayer under different strains.

ing solution and the LSDA+ U HM solution [Fig. 3(b)], one might infer that it is the SOC which opens the band gap. However, this is a wrong statement. How can the SOC (a few tens of meV in strength) open the gap more than 1 eV ? Actually, here the SOC offers new orbital degrees of freedom, and the Hubbard U determines the band gap. The semiconducting $d^{5\uparrow}a_{1g}^{\downarrow}$ solution remains almost unchanged by a comparison between Figs. 3(a) and 4(b), and this solution is less stable than the $d^{5\uparrow}l_{z+}^{\downarrow}$ ground state by about 85 meV/fu , see Table 1.

The $d^{5\uparrow}l_{z+}^{\downarrow}$ ground state has the orbital moment of $0.59 \mu_B$ along the z axis, in addition to the spin moment of $3.56 \mu_B$. It has the easy perpendicular magnetization and is more stable than the planar magnetization by 13.43 meV/Fe , see Table 1. Therefore, the total magnetic moment of $4.15 \mu_B/\text{Fe}$ along the z axis well accounts for the experimental perpendicular moment of $4.3 \mu_B$ [27, 29, 30]. Moreover, the $d^{5\uparrow}l_{z+}^{\downarrow}$ ground state prefers a FM coupling in FeCl_2 monolayer, and it is more stable than the stripe AF state by 2.83 meV/Fe . Using the magnetic exchange expressions $-JS^2$ for each FM pair with $S = 2$, $-3JS^2$ per fu for the FM state, and JS^2 per fu for the stripe AF state, we derive the FM exchange parameter $J = 2.83/4S^2 \approx 0.18 \text{ meV}$. In addition, for the metastable $d^{5\uparrow}a_{1g}^{\downarrow}$ state, the SOC mixes the nearly degenerate a_{1g} and e'_g states and produces a planar orbital moment of $0.23 \mu_B$. Note that this easy planar magnetization would fail to explain the experimental perpendicular magnetization. Therefore, all the above LSDA+SOC+ U results lead us to a conclusion that $d^{5\uparrow}l_{z+}^{\downarrow}$ (but not $d^{5\uparrow}a_{1g}^{\downarrow}$) is the correct ground state and it consistently explains the FM semiconducting behavior of FeCl_2 monolayer with the perpendicular magnetization.

In order to estimate the T_C of FeCl_2 monolayer, we

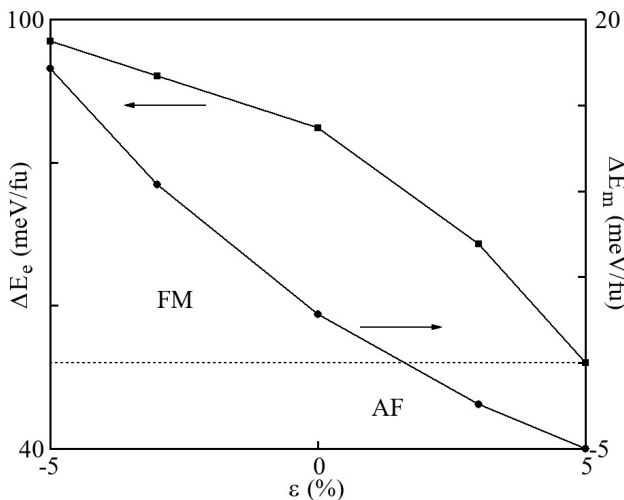


FIG. 6. ΔE_e (meV/fu): the relative stability of the $d^{5\uparrow}l^1_{z+}$ ground state against the $d^{5\uparrow}a^1_{1g}$ state under different strains. ΔE_m (meV/fu): the $d^{5\uparrow}l^1_{z+}$ FM state against the AF state.

assume the spin Hamiltonian and carry out Monte Carlo simulations

$$H = -\frac{J}{2} \sum_{\langle ij \rangle} \vec{S}_i \cdot \vec{S}_j - D \sum_i (S_i^z)^2,$$

where the first term represents the isotropic Heisenberg exchange with $J = 0.18$ meV, and the D parameter in the second term stands for the magnetic anisotropy of the single ion type. Our LSDA+SOC+ U results listed in Table 1 suggest the easy z -axis magnetization with the anisotropy energy of 13.43 meV/Fe and $S_z = 2$, and thus $D = 3.36$ meV can be derived. Using these J and D parameters, our Monte Carlo simulations give $T_C = 25$ K for the pristine FeCl₂ monolayer, see Fig. 5.

As a lattice strain is an effective way to tune the electronic state and magnetism of 2D materials, here we also study a biaxial strain effect on the FM of FeCl₂ monolayer. A compressive strain would raise the crystal field level of the a_{1g} singlet, and thus further stabilizes the $d^{5\uparrow}l^1_{z+}$ ground state. As shown in Table 1 and Fig. 6,

the 3% or 5% compressive strain gives a larger orbital moment, a stronger perpendicular anisotropy, and a stronger FM coupling, according to the LSDA+SOC+ U calculations. Therefore, the T_C is naturally expected to be enhanced, and this is indeed confirmed by our Monte Carlo simulations (see Fig. 5): T_C is 69 K for the -3% strain and 102 K for -5% strain. In addition, we study a tensile strain, which would gradually destabilize the $d^{5\uparrow}l^1_{z+}$ ground state. Our LSDA+SOC+ U calculations show that the orbital moment gets smaller, the perpendicular magnetic anisotropy shrinks, and strikingly, the intralayer magnetic coupling changes its sign: the stripe AF state gets more stable than the FM state upon 3% and 5% strain. All these results show that a compressive strain would significantly enhance the T_C of FeCl₂ monolayer, but that a tensile strain could trigger an interesting FM-AF transition. Therefore, FeCl₂ monolayer could be an appealing 2D magnetic semiconductor potentially suitable for spintronic applications.

IV. CONCLUSIONS

In summary, using a set of delicate DFT calculations including the SOC and Hubbard U , aided with the crystal field level analyses, we achieve the correct $d^{5\uparrow}l^1_{z+}$ ground state for FeCl₂ monolayer. This ground state well explains, in a consistent way, the experimental FM semiconducting behavior with the perpendicular magnetization, and our Monte Carlo simulation gives $T_C = 25$ K for the pristine FeCl₂ monolayer. Moreover, we find that upon the compressive strain, the $d^{5\uparrow}l^1_{z+}$ ground state gets more stable, and the enhanced FM coupling and the perpendicular magnetic anisotropy raise the T_C a lot, up to 69 K (102 K) for -3% (-5%) strain. We also predict an interesting FM-AF transition for FeCl₂ monolayer under a tensile strain. All these results suggest that FeCl₂ monolayer is an appealing 2D magnetic semiconductor.

V. ACKNOWLEDGEMENTS

This work was supported by National Natural Science Foundation of China (Grants No. 12104307 and No. 12174062).

-
- [1] K. S. Novoselov, A. K. Geim, S. V. Morozov, D. Jiang, Y. Zhang, S. V. Dubonos, I. V. Grigorieva, and A. A. Firsov, *Sci. Rep.* **306**, 5 (2004).
- [2] K. S. Novoselov, A. K. Geim, S. V. Morozov, D. Jiang, M. I. Katsnelson, I. V. Grigorieva, S. V. Dubonos, and A. A. Firsov, *Nature* **438**, 197 (2005).
- [3] Y. Zhang, Y.-W. Tan, H. L. Stormer, and P. Kim, *Nature* **438**, 201 (2005).
- [4] Y. Cao, V. Fatemi, S. Fang, K. Watanabe, T. Taniguchi, E. Kaxiras, and P. Jarillo-Herrero, *Nature* **556**, 43 (2018).
- [5] Z. Sun, Y. Yi, T. Song, G. Clark, B. Huang, Y. Shan, S. Wu, D. Huang, C. Gao, Z. Chen, M. McGuire, *et al.*, *Nature* **572**, 497 (2019).
- [6] N. D. Mermin and H. Wagner, *Phys. Rev. Lett.* **17**, 1133 (1966).
- [7] B. Huang, G. Clark, E. Navarro-Moratalla, D. R. Klein, R. Cheng, K. L. Seyler, D. Zhong, E. Schmidgall, M. A. McGuire, D. H. Cobden, *et al.*, *Nature* **546**, 270 (2017).

- [8] C. Gong, L. Li, Z. Li, H. Ji, A. Stern, Y. Xia, T. Cao, W. Bao, C. Wang, Y. Wang, *et al.*, *Nature* **546**, 265 (2017).
- [9] D.-H. Kim, K. Kim, K.-T. Ko, J. Seo, J. S. Kim, T.-H. Jang, Y. Kim, J.-Y. Kim, S.-W. Cheong, and J.-H. Park, *Phys. Rev. Lett.* **122**, 207201 (2019).
- [10] K. Yang, F. Fan, H. Wang, D. Khomskii, and H. Wu, *Phys. Rev. B* **101**, 100402 (2020).
- [11] L. Liu, K. Yang, G. Wang, and H. Wu, *J. Mater. Chem. C* **8**, 14782 (2020).
- [12] C. Xu, J. Feng, M. Kawamura, Y. Yamaji, Y. Nahas, S. Prokhorenko, Y. Qi, H. Xiang, and L. Bellaiche, *Phys. Rev. Lett.* **124**, 087205 (2020).
- [13] Y. Gong, J. Guo, J. Li, K. Zhu, M. Liao, X. Liu, Q. Zhang, L. Gu, L. Tang, X. Feng, *et al.*, *Chinese Phys. Lett.* **36**, 076801 (2019).
- [14] Y. Deng, Y. Yu, M. Z. Shi, Z. Guo, Z. Xu, J. Wang, X. H. Chen, and Y. Zhang, *Science* **367**, 895 (2020).
- [15] M. M. Otrokov, I. I. Klimovskikh, H. Bentmann, D. Estyunin, A. Zeugner, Z. S. Aliev, S. Gaß, A. U. B. Wolter, A. V. Koroleva, A. M. Shikin, *et al.*, *Nature* **576**, 416 (2019).
- [16] C. Cardoso, D. Soriano, N. García-Martínez, and J. Fernández-Rossier, *Phys. Rev. Lett.* **121**, 067701 (2018).
- [17] D. R. Klein, D. MacNeill, J. L. Lado, D. Soriano, E. Navarro-Moratalla, K. Watanabe, T. Taniguchi, S. Manni, P. Canfield, J. Fernández-Rossier, *et al.*, *Science* **360**, 1218 (2018).
- [18] T. Song, X. Cai, M. W.-Y. Tu, X. Zhang, B. Huang, N. P. Wilson, K. L. Seyler, L. Zhu, T. Taniguchi, K. Watanabe, *et al.*, *Science* **360**, 1214 (2018).
- [19] A. Soumyanarayanan, N. Reyren, A. Fert, and C. Panagopoulos, *Nature (London)* **539**, 509 (2016).
- [20] Y. Deng, Y. Yu, Y. Song, J. Zhang, N. Z. Wang, Z. Sun, Y. Yi, Y. Z. Wu, S. Wu, J. Zhu, *et al.*, *Nature (London)* **563**, 94 (2018).
- [21] C. Huang, J. Feng, F. Wu, D. Ahmed, B. Huang, H. Xiang, K. Deng, and E. Kan, *J. Am. Chem. Soc.* **140**, 11519 (2018).
- [22] M. Gibertini, *Nat. Nanotechnol.* **14**, 12 (2019).
- [23] S. Liu, K. Yang, W. Liu, E. Zhang, Z. Li, X. Zhang, Z. Liao, W. Zhang, J. Sun, Y. Yang, *et al.*, *Natl. Sci. Rev.* **7**, 745 (2020).
- [24] B. Huang, G. Clark, D. R. Klein, D. MacNeill, E. Navarro-Moratalla, K. L. Seyler, N. Wilson, M. A. McGuire, D. H. Cobden, D. Xiao, *et al.*, *Nat. Nanotechnol.* **13**, 544 (2018).
- [25] S. Jiang, J. Shan, and K. F. Mak, *Nat. Mater.* **17**, 406 (2018).
- [26] M. McGuire, *Crystals* **7**, 121 (2017).
- [27] M. K. Wilkinson, J. W. Cable, E. O. Wollan, and W. C. Koehler, *Phys. Rev.* **113**, 497 (1959).
- [28] M. E. Lines, *Phys. Rev.* **131**, 546 (1963).
- [29] R. J. Birgeneau, W. B. Yelon, E. Cohen, and J. Makovsky, *Phys. Rev. B* **5**, 2607 (1972).
- [30] I. Jacobs and P. Lawrence, *Phys. Rev.* **164**, 866 (1967).
- [31] X. Zhou, B. Brzostowski, A. Durajski, M. Liu, J. Xiang, T. Jiang, Z. Wang, S. Chen, P. Li, Z. Zhong, A. Drzewiński, *et al.*, *J. Phys. Chem. C* **124**, 9416 (2020).
- [32] S. Cai, F. Yang, and C. Gao, *Nanoscale* **12**, 16041 (2020).
- [33] E. Torun, H. Sahin, S. K. Singh, and F. M. Peeters, *Appl. Phys. Lett.* **106**, 192404 (2015).
- [34] M. Ashton, D. Gluhovic, S. B. Sinnott, J. Guo, D. A. Stewart, and R. G. Hennig, *Nano Lett.* **17**, 5251 (2017).
- [35] Y. Feng, X. Wu, J. Han, and G. Gao, *J. Mater. Chem. C* **6**, 4087 (2018).
- [36] V. V. Kulish and W. Huang, *J. Mater. Chem. C* **5**, 8734 (2017).
- [37] R. K. Ghosh, A. Jose, and G. Kumari, *Phys. Rev. B* **103**, 054409 (2021).
- [38] A. S. Botana and M. R. Norman, *Phys. Rev. Materials* **3**, 044001 (2019).
- [39] Q. Yao, J. Li, and Q. Liu, *Phys. Rev. B* **104**, 035108 (2021).
- [40] P. Blaha, K. Schwarz, G. Madsen, D. Kvasnicka, J. Luitz, R. Laskowski, F. Tran, and L. Marks, “Wien2k software package,” (2001).
- [41] V. I. Anisimov, I. Solovyev, M. Korotin, M. Czyżyk, and G. Sawatzky, *Phys. Rev. B* **48**, 16929 (1993).
- [42] J. P. Perdew and A. Zunger, *Phys. Rev. B* **23**, 5048 (1981).
- [43] R. Shinde, S. S. Yamijala, and B. M. Wong, *J. Phys.: Condens. Matter* **33**, 115501 (2021).
- [44] A. D. Becke, *J. Chem. Phys.* **98**, 1372 (1993).
- [45] B. Andriyevsky and K. Doll, *J. Phys. Chem. Solids* **70**, 84 (2009).
- [46] M. van Schilfgaarde, T. Kotani, and S. Faleev, *Phys. Rev. Lett.* **96**, 226402 (2006).
- [47] N. Metropolis and S. Ulam, *J. Am. Stat. Assoc.* **44**, 335 (1949).
- [48] H. Wu, M. Haverkort, Z. Hu, D. Khomskii, and L. Tjeng, *Phys. Rev. Lett.* **95**, 186401 (2005).
- [49] X. Ou and H. Wu, *Sci. Rep.* **4**, 4609 (2014).